

# Weierstrass meets Enriques

A. P. Braun, R. Ebert, A. Hebecker, R. Valandro

*Institut für Theoretische Physik, Universität Heidelberg,  
Philosophenweg 16-19, 69120 Heidelberg, Germany* \*

## Abstract

We study in detail the degeneration of  $K3$  to  $T^4/\mathbb{Z}_2$ . We obtain an explicit embedding of the lattice of collapsed cycles of  $T^4/\mathbb{Z}_2$  into the lattice of integral cycles of  $K3$  in two different ways. Our first method exploits the duality to the heterotic string on  $T^3$ . This allows us to describe the degeneration in terms of Wilson lines. Our second method is based on the blow-up of  $T^4/\mathbb{Z}_2$ . From this blow-up, we directly construct the full lattice of integral cycles of  $K3$ . Finally, we use our results to describe the action of the Enriques involution on elliptic  $K3$  surfaces, finding that a Weierstrass model description is consistent with the Enriques involution only in the F-theory limit.

---

\*a.braun, a.hebecker, r.valandro @thphys.uni-heidelberg.de, email@rainerebert.de

# Contents

<b>1</b>	<b>Introduction</b>	<b>2</b>
<b>2</b>	<b>The lattice <math>E_8</math> and its sublattice <math>A_1^{\oplus 8}</math></b>	<b>4</b>
<b>3</b>	<b>Moduli space of <math>K3</math> and Wilson line breaking</b>	<b>7</b>
<b>4</b>	<b>The <math>T^4/\mathbb{Z}_2</math> orbifold limit of <math>K3</math></b>	<b>9</b>
<b>5</b>	<b><math>T^4/\mathbb{Z}_2</math> as a double cover of <math>\mathbb{P}^1 \times \mathbb{P}^1</math></b>	<b>13</b>
5.1	Divisors and cycles in the blow-up of $T^4/\mathbb{Z}_2$ . . . . .	15
5.2	Juxtaposition . . . . .	18
<b>6</b>	<b>The Enriques involution</b>	<b>20</b>
6.1	The standard Weierstrass model . . . . .	21
6.2	A symmetric Weierstrass model . . . . .	25
<b>7</b>	<b>F-theory Limit</b>	<b>26</b>
<b>8</b>	<b>Conclusions and Outlook</b>	<b>29</b>
<b>A</b>	<b>Explicit expressions for the <math>\sigma_{ij}^k</math></b>	<b>30</b>

## 1 Introduction

In the study of string-theory compactifications, the geometric understanding of the cycle structure of complex manifold plays a central role. Examples are F-theory models with fluxes (see e.g. [1] for a review and [2–10] for recent work) and blow-ups of heterotic orbifolds (see e.g. [11–15]). One of the simplest relevant geometries, which may also play a role as a building block in more complex models, is the  $K3$  surface [16–18].

Shrinking sixteen two-spheres in  $K3$ , the surface develops sixteen  $A_1$  singularities. This corresponds to the  $T^4/\mathbb{Z}_2$  orbifold limit. To describe this degeneration in detail, we need to know which two-spheres shrink. The answer to this question represents our central result: We construct an embedding of the cycles of  $T^4/\mathbb{Z}_2$ , including the lattice  $A_1^{\oplus 16}$  of collapsed cycles, into the lattice  $\Gamma_{3,19} = U^{\oplus 3} \oplus (-E_8)^{\oplus 2}$  of integral cycles of  $K3$ . This embedding yields an elegant description of  $\Gamma_{3,19}$  making all the symmetries of  $T^4/\mathbb{Z}_2$  manifest. It

also allows for a rather intuitive understanding of the cycle structure and certain regions of the moduli space of  $K3$ , which is based on the possibility to visualize  $T^4/\mathbb{Z}_2$  using a four-dimensional hypercube.

Furthermore, we are interested in the action of the Enriques involution<sup>1</sup> on elliptic  $K3$  surfaces, especially its compatibility with the description of  $K3$  by a Weierstrass model. The Weierstrass model is of particular interest as it is commonly used in the context of F-theory [21, 22]. It is known that  $T^4/\mathbb{Z}_2$  allows an Enriques involution [23]. Using the results of the first part of this paper, we show how to deform  $T^4/\mathbb{Z}_2$  to a  $K3$  given by the standard Weierstrass form. It turns out that this deformation is not consistent with the *holomorphicity* of the Enriques involution, the obstacle being the single distinguished section of the Weierstrass model<sup>2</sup>. This problem does not arise for elliptic  $K3$  surfaces that are given in non-standard Weierstrass form, e.g. one with two distinguished sections [24, 25]. In the F-theory limit, however, also the usual Weierstrass form becomes symmetric under the Enriques involution.

This paper is organized as follows:

In Sects. 2 and 3, we explicitly work out the equivalence between the resolution of singularities of  $K3$  and Wilson line breaking of  $E_8 \times E_8$ . In particular, we show that the relevant breaking of  $E_8$  to  $SU(2)^8$  is highly symmetric: It is achieved by three Wilson lines which are all equivalent through automorphisms of the  $E_8$  lattice.

Sect. 4 combines the results of the previous two sections and identifies the integral cycles of  $K3$  which shrink to produce the sixteen  $A_1$  singularities. Furthermore, we reproduce the known action of the Enriques involution on  $T^4/\mathbb{Z}_2$  [23] from its action on  $H_2(K3, \mathbb{Z})$  as given in the mathematics literature [19].

In Sect. 5, we describe  $K3$  and in particular  $T^4/\mathbb{Z}_2$  as a double cover of  $\mathbb{P}^1 \times \mathbb{P}^1$ . This description nicely displays holomorphic sections and shows which of the singularities they hit.

We then construct the full lattice  $H_2(K3, \mathbb{Z})$  in a blow-up of  $T^4/\mathbb{Z}_2$  in Sect. 5.1. Our starting point are the six even cycles of  $T^4$  and the sixteen exceptional divisors emerging in the blow-up of the singularities. While these cycles span  $H_2(K3, \mathbb{R})$  as a real vector space, they do not form an integral basis of  $H_2(K3, \mathbb{Z})$ . We construct the extra integral cycles which complete the lattice  $U(2)^{\oplus 3} \oplus A_1^{\oplus 16}$  to  $U^{\oplus 3} \oplus (-E_8)^{\oplus 2}$ . The structure of this

---

<sup>1</sup>The Enriques involution is a fixed-point free holomorphic involution of  $K3$  which is non-symplectic, i.e. it projects out the holomorphic two-form [19, 20]. It yields the Enriques surface as the quotient space.

<sup>2</sup> A freely acting  $\mathbb{Z}_2$ -symmetry of the real metric manifold still exists, but it is not holomorphic in the complex structure of the Weierstrass model.

complete lattice can be nicely displayed in terms of a four-dimensional cube. This provides an intuitive geometrical picture of the cycles of  $K3$ .

We demonstrate the equivalence between the two embeddings of  $A_1^{\oplus 16}$  into  $\Gamma_{3,19}$  in Sect. 5.2 by finding an explicit map between them.

In Sect. 6 we relate the action of the Enriques involution on  $T^4/\mathbb{Z}_2$  to its action on the lattice of integral cycles of  $K3$ . We proceed by showing that elliptic  $K3$  surfaces described by the standard Weierstrass model do not allow an Enriques involution. It turns out that the Enriques involution requires the existence of at least two holomorphic sections (which are mapped to each other).

In Sect. 7 we finally discuss the F-theory limit of  $T^4/\mathbb{Z}_2$  and of elliptic  $K3$ s described by a Weierstrass model with one or two distinguished sections. Even though these spaces are different and correspond to different M-theory compactifications, they yield equivalent models in the F-theory limit in which the fibre of the elliptic fibrations is collapsed<sup>3</sup>. This means in particular that in this limit the standard Weierstrass model becomes symmetric under the Enriques involution.

## 2 The lattice $E_8$ and its sublattice $A_1^{\oplus 8}$

The  $E_8$  root lattice is the unique even unimodular lattice of rank 8. Any element takes the form  $\alpha = q_I E_I$ , where  $\{E_I\}_{I=1,\dots,8}$  is a basis of  $\mathbb{R}^8$  satisfying  $E_I \cdot E_J = -\delta_{IJ}$ . The coordinates have to be all integer or half-integer and must fulfill  $\sum_{I=1,\dots,8} q_I = 2\mathbb{Z}$  [27]. Thus the lattice is generated by vectors of the type

$$(\pm 1, \pm 1, 0, 0, 0, 0, 0, 0) \quad \text{and} \quad \left(\pm \frac{1}{2}, \pm \frac{1}{2}, \pm \frac{1}{2}, \pm \frac{1}{2}, \pm \frac{1}{2}, \pm \frac{1}{2}, \pm \frac{1}{2}, \pm \frac{1}{2}\right),$$

where the second type of vectors must have an even number of minus signs. We choose the (non-unique) set of 8 simple roots

$$\begin{aligned} \alpha_1 &= \frac{1}{2}E_1 + \frac{1}{2}E_2 + \dots + \frac{1}{2}E_8 & \alpha_5 &= -E_4 + E_5 \\ \alpha_2 &= -E_7 - E_8 & \alpha_6 &= -E_3 + E_4 \\ \alpha_3 &= -E_6 + E_7 & \alpha_7 &= -E_2 + E_3 \\ \alpha_4 &= -E_5 + E_6 & \alpha_8 &= -E_7 + E_8. \end{aligned} \tag{1}$$

---

<sup>3</sup>This is clear since our models have the same constant  $\tau$  as a function of the base, and this fact is the only feature of the fibration that is relevant in F-theory, see e.g. [26]

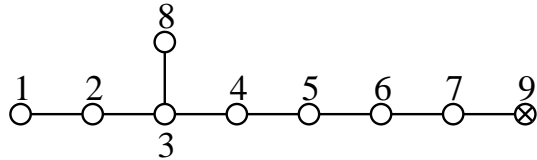


Figure 1: The extended Dynkin diagram of  $E_8$ .

The structure of this basis is encoded in the *Dynkin diagram* of  $E_8$ . The *extended Dynkin diagram* is obtained by adding the (linearly dependent and thus non-simple) highest root [28] (see Fig. 1).

$$\alpha_9 = -2\alpha_1 - 4\alpha_2 - 6\alpha_3 - 5\alpha_4 - 4\alpha_5 - 3\alpha_6 - 2\alpha_7 - 3\alpha_8 = -E_1 + E_2. \quad (2)$$

The coefficients in this expansion are known as the *Coxeter labels*.

The reflections in the hyperplanes orthogonal to the 240 roots are symmetries of the  $E_8$  root lattice and generate the Weyl group of type  $E_8$ . Its order is given by  $4! \cdot 6! \cdot 8! = 696729600$  [27]. The  $E_8$  Weyl group contains a subgroup of order  $8! \cdot 2^7$  consisting of all permutations of the coordinates and all even sign changes. This subgroup is the Weyl group of type  $D_8$ . The full  $E_8$  Weyl group is generated by this subgroup and the block diagonal matrix  $\mathcal{H}_4 \oplus \mathcal{H}_4$  where  $\mathcal{H}_4$  is the Hadamard matrix

$$\mathcal{H}_4 = \frac{1}{2} \begin{pmatrix} 1 & 1 & 1 & 1 \\ 1 & -1 & 1 & -1 \\ 1 & 1 & -1 & -1 \\ 1 & -1 & -1 & 1 \end{pmatrix}. \quad (3)$$

In gauge field theories based on a certain group, the symmetry can be broken by introducing Wilson lines associated with non-contractible loops of the underlying space-time geometry. This is in one-to-one correspondence with Dynkin's method for finding maximal subgroups by deleting nodes in the extended Dynkin diagram.

The action of a Wilson line in  $E_8$  (viewed as a vector in  $\mathbb{R}^8$ ) on a root  $\alpha$  is

$$\alpha \mapsto e^{2\pi i \alpha \cdot W} \alpha. \quad (4)$$

To find the sublattice of  $E_8$  which corresponds to deleting a simple root  $\alpha_i$ , we choose a Wilson line  $W$  satisfying (see, e.g., [29, 30])

$$\alpha_i \cdot W \notin \mathbb{Z} \quad \text{and} \quad \alpha_j \cdot W \in \mathbb{Z} \quad \text{for } j \in \{1, \dots, 9\} \setminus \{i\}. \quad (5)$$

Requiring this transformation to be a symmetry of the root lattice, we are left with the

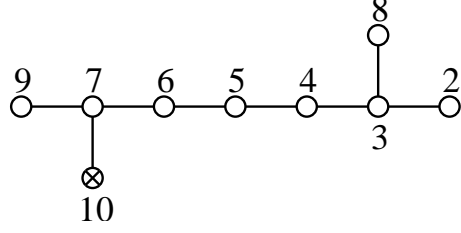


Figure 2: The extended Dynkin diagram of  $D_8$ .

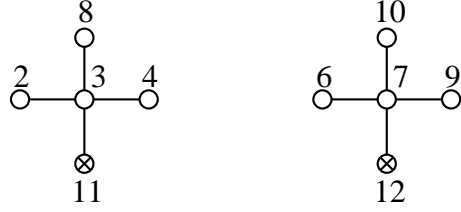


Figure 3: Twice the extended Dynkin diagram of  $D_4$ .

sublattice of roots satisfying  $\alpha \cdot W \in \mathbb{Z}$  [31, 32]. In the following we will show that

$$W^1 = (1, 0^7), \quad W^2 = (0^4, -\frac{1}{2}^4) \quad \text{and} \quad W^3 = (0^2, -\frac{1}{2}, \frac{1}{2}, 0^2, -\frac{1}{2}, \frac{1}{2}) \quad (6)$$

take us from  $E_8$  to  $A_1^{\oplus 8}$ .

It is easy to see that these three Wilson lines are equivalent, i.e. they are related by a Weyl reflection<sup>4</sup>.

Let us start with  $W^1$ . This Wilson line removes  $\alpha_1$ , giving us the Dynkin diagram of  $D_8$ . Adding the highest root of the  $D_8$  lattice,

$$\alpha_{10} = -\alpha_2 - 2\alpha_3 - 2\alpha_4 - 2\alpha_5 - 2\alpha_6 - 2\alpha_7 - \alpha_8 - \alpha_9 = E_1 + E_2 .$$

we obtain the extended Dynkin diagram of  $D_8$  (see Fig. 2).

Next,  $W^2$  removes the node corresponding to  $\alpha_5$ . We are left with two copies of the Dynkin diagram of  $D_4$  (see Fig. 3), which we extend by their respective highest roots

$$\alpha_{11} = -\alpha_2 - 2\alpha_3 - \alpha_4 - \alpha_8 = E_5 + E_6 \quad \text{and} \quad \alpha_{12} = -\alpha_6 - 2\alpha_7 - \alpha_9 - \alpha_{10} = -E_3 - E_4 .$$

---

<sup>4</sup>For example, if we apply  $\mathcal{H}_4 \oplus \mathcal{H}_4$  and the following element of the Weyl subgroup of type  $D_8$ ,  $(E_1, E_2, E_3, E_4, E_5, E_6, E_7, E_8) \mapsto (-E_3, E_8, E_4, -E_7, -E_1, E_6, E_2, -E_5)$ , we get  $W^1 \mapsto W^3$ ,  $W^2 \mapsto W^1$  and  $W^3 \mapsto W^2$ .

Finally,  $W^3$  removes  $\alpha_3$  and  $\alpha_7$ , leaving us with 8 unconnected nodes corresponding to the  $A_1^{\oplus 8}$  sublattice of  $E_8$ .<sup>5</sup> The remaining simple roots are:

$$\begin{aligned} \alpha_2 &= -E_7 - E_8 & \alpha_4 &= -E_5 + E_6 & \alpha_6 &= -E_3 + E_4 & \alpha_8 &= -E_7 + E_8 \\ \alpha_9 &= -E_1 + E_2 & \alpha_{10} &= E_1 + E_2 & \alpha_{11} &= E_5 + E_6 & \alpha_{12} &= -E_3 - E_4 \end{aligned} \quad (7)$$

### 3 Moduli space of $K3$ and Wilson line breaking

Up to diffeomorphisms,  $K3$  is the only non-trivial compact Calabi-Yau twofold.<sup>6</sup> Its second homology class  $H_2(K3, \mathbb{Z})$ , equipped with the natural metric given by the intersection numbers between cycles, is an even, self-dual lattice with signature  $(3, 19)$ , commonly denoted by  $\Gamma_{3,19}$ . There is a basis of  $H_2(K3, \mathbb{Z})$  such that the matrix formed by the inner products of the basis vectors reads

$$U \oplus U \oplus U \oplus (-E_8) \oplus (-E_8), \quad (8)$$

where  $E_8$  is the positive definite Cartan matrix of  $E_8$  and

$$U = \begin{pmatrix} 0 & 1 \\ 1 & 0 \end{pmatrix}.$$

We will denote the basis vectors spanning the three  $U$  blocks by  $e_i$  and  $e^i$ ,  $i = 1, 2, 3$ . Accordingly,  $e^i \cdot e_j = \delta_j^i$ . Using the notation introduced in the last section for the  $E_8$  lattice, any integral 2-cycle can now be written as

$$p^i e^i + p_i e_i + q_I E_I, \quad (9)$$

where  $i = 1, 2, 3$  and  $I = 1, \dots, 16$ . The  $p_i$  as well as the  $p^i$  are all integers, while the  $q_I$  fulfill the relations  $\sum_{I=1, \dots, 8} q_I = 2\mathbb{Z}$  and  $\sum_{I=9, \dots, 16} q_I = 2\mathbb{Z}$  and furthermore have to be *all* integer or *all* half-integer in each of the two  $E_8$  blocks.

A point in the moduli space  $M_{K3}$  of  $K3$  is chosen by fixing the overall volume of  $K3$  and a positive signature 3-plane  $\Sigma$  in  $H_2(K3, \mathbb{R}) \cong \mathbb{R}^{3,19}$ . We choose three real 2-cycles  $\omega_i \in H_2(K3, \mathbb{R})$ ,  $i = 1, 2, 3$ , which fulfill the constraints  $\omega_i \cdot \omega_j = \delta_{ij}$  and span  $\Sigma$ . A real

---

<sup>5</sup>Here, the removed nodes are two instead of one; this is because the Wilson line acts on two simple groups.

<sup>6</sup>For a comprehensive review of  $K3$ , see [16].

Kähler form  $j$  and a holomorphic two-form  $\omega$  for the  $K3$  surface specified by  $\Sigma$  are then given by  $j = \sqrt{2 \cdot \text{Vol}(K3)} \cdot \omega_3$  and  $\omega = \omega_1 + i\omega_2$ , respectively<sup>7</sup>.

The roots of  $\Gamma_{3,19}$  are defined as the elements of  $H_2(K3, \mathbb{Z})$  with self-intersection  $-2$ . If a root becomes orthogonal to  $\Sigma$ , the  $K3$  surface develops a singularity since the corresponding 2-cycle shrinks<sup>8</sup>.

For example, a  $\mathbb{C}^2/\mathbb{Z}_2$  singularity (also called  $A_1$  singularity) arises if a single root shrinks. In general, the singularities which can occur are of A-D-E type and are specified by the simple roots in the orthogonal complement of  $\Sigma$ . The intersection matrix of the cycles corresponding to these roots can be shown to always be minus the Cartan matrix of some A-D-E group [16, 19]. This group uniquely determines the A-D-E-type singularity of the  $K3$  surface given by  $\Sigma$ .

The  $E_8 \times E_8$  point in moduli space is realized when  $\Sigma$  is located in the  $U^{\oplus 3}$  block spanned by  $e_i, e^i$  ( $i = 1, 2, 3$ )<sup>9</sup>. Rotating the plane into the  $E_8 \times E_8$  block changes the singularity and eventually gives rise to a smooth  $K3$ . Singularities which may still be present after this rotation correspond to subgroups of  $E_8 \times E_8$ . As we explain in detail in the following, one can relate the symmetry breaking by Wilson lines described in Sect. 2 to the rotation of the  $\Sigma$  plane in  $H_2(K3, \mathbb{R})$ .

We first consider the rotation of  $\Sigma$  from a point with  $E_8 \times E_8$  singularity to a point with  $D_8 \times E_8$  singularity. The Wilson line that realizes this breaking is  $W_I = (1, 0, 0, 0, 0, 0, 0, 0)$  (see Sect. 2). This identifies a vector  $W = W_I E_I = (1, 0, 0, 0, 0, 0, 0, 0)$  in the subspace of  $H_2(K3, \mathbb{R})$  that corresponds to the first  $E_8$  block in (8). Let us now rotate  $\Sigma$  in the direction of  $W$ . We can do this by rotating one of basis vectors of  $U^{\oplus 3}$  (where  $\Sigma$  lives), e.g.  $e^1$ , in this direction:  $e^1 \rightarrow e^1 + \beta W$ ,  $\beta \in \mathbb{R}$ . Once this rotation has been performed,  $\Sigma$  is located in the subspace of  $H_2(K3, \mathbb{R})$  spanned by

$$e_1, \quad e^1 + \beta W, \quad e_2, \quad e^2, \quad e_3, \quad e^3. \quad (10)$$

For a generic position of  $\Sigma$  in this six dimensional space and for generic values of  $\beta$ , the lattice  $\Lambda$  orthogonal to  $\Sigma$  is of the type  $D_7 \times E_8$ .<sup>10</sup> Reinterpreting (1) as a set of simple roots of  $\Gamma_{E_8 \times E_8}$ , this can be understood from the fact that the cycle corresponding to  $\alpha_1$  as well as the cycle corresponding to the highest root (2) acquire finite volume. For  $\beta = 1$ , we

---

<sup>7</sup>Here and below, we use the same character for a 2-form, its associated cohomology class and its Poincaré-dual 2-cycle.

<sup>8</sup>The volume of a 2-cycle  $\gamma$  is proportional to its projection on  $\Sigma$ .

<sup>9</sup>Accordingly,  $\omega_i^{E_8 \times E_8} = a_i^j e_j + b_k^i e^k$ ,  $i, j, k = 1, 2, 3$ , for real numbers  $a_i^j$  and  $b_k^i$  s.t.  $\omega_i \cdot \omega_j = \delta_{ij}$ .

<sup>10</sup>In M-theory on the  $K3$  surface given by  $\Sigma$  this leads to the gauge group  $SO(14) \times U(1) \times E_8$ .



find that  $\alpha_9 + e_1$  is orthogonal to  $e^1 + \beta W$  (and hence to  $\Sigma$ ) and we therefore have a further independent shrinking cycle. This results in a change of singularity type to  $D_8 \times E_8$ .<sup>11</sup> The fact that we found another shrinking cycle is due to the integrality of  $\alpha_9 \cdot W$ . Thus the orthogonality of  $\alpha_9 + e_1$  to  $e^1 + \beta W$  for  $\beta = 1$  corresponds to the previously discussed condition for the highest root to survive after introducing the Wilson line  $\beta W_I$ .

This reasoning can be extended to a generic rotation of  $\Sigma$  into the  $E_8 \times E_8$  block. In the most general case, three vectors  $W^i$  are introduced and every orbifold point in  $M_{K3}$  can be reached. All of this is expected, given the well known duality between M-theory compactified on  $K3$  and the heterotic string compactified on  $T^3$  [16, 33]. The  $W^i$  are the three Wilson lines that can be used to break the gauge symmetry on the heterotic side.

## 4 The $T^4/\mathbb{Z}_2$ orbifold limit of $K3$

We begin with some definitions regarding  $T^4/\mathbb{Z}_2$ . The non-trivial element of  $\mathbb{Z}_2$  acts as  $-1$  on all the coordinates  $x_i$  ( $i = 1, \dots, 4$ ) of  $T^4$ . After modding out, the 16 points of  $T^4$  fixed under the  $\mathbb{Z}_2$ -action lead to 16  $A_1$  singularities. Their locations are at

$$(x_1, x_2, x_3, x_4) = (\xi_1, \xi_2, \xi_4, \xi_4), \quad \text{with} \quad \xi_i = 0, \frac{1}{2}. \quad (11)$$

The 2-cycles of  $T^4$  are all even with respect to  $\mathbb{Z}_2$  and survive the orbifolding. An integral basis is given by the six 2-tori  $\pi_{ij}$  corresponding to the  $x_i$ - $x_j$ -plane. Their intersection numbers are

$$\pi_{ij} \cdot \pi_{ml} = 2\epsilon_{ijml}. \quad (12)$$

The corresponding Poincaré-dual 2-forms are

$$\text{PD}[\pi_{ij}] = \epsilon_{ijpq} dx_p \wedge dx_q. \quad (13)$$

As we will see in more details later, blowing up the 16  $A_1$  singularities of  $T^4/\mathbb{Z}_2$  gives rise to 16  $\mathbb{P}^1$ s. They are orthogonal with respect to each other and to the torus-cycles  $\pi_{ij}$ . There is a natural choice of complex structure on  $T^4/\mathbb{Z}_2$ :  $z_1 = x_1 + \tau_1 x_4$  and  $z_2 = x_2 + \tau_2 x_3$ <sup>12</sup>.

<sup>11</sup>This corresponds to gauge enhancement  $SO(16) \times E_8$  in M-theory.

<sup>12</sup>The natural expressions for the Kähler form  $j$  and the holomorphic two-form  $\omega$  are then  $\omega = dz_1 \wedge dz_2$  and  $j = a_1 dz_1 \wedge d\bar{z}_1 + a_2 dz_2 \wedge d\bar{z}_2 + \text{Re}[b dz_1 \wedge \bar{z}_2]$ , where  $a_1, a_2 \in \mathbb{R}$  and  $b \in \mathbb{C}$ . In terms of the Poincaré-dual of the integral cycles  $\pi_{ij}$ , we have

$$\omega = \pi_{34} + \tau_1 \pi_{13} + \tau_2 \pi_{42} - \tau_1 \tau_2 \pi_{12} \quad j = \hat{a}_1 \pi_{23} + \hat{a}_2 \pi_{14} + \text{Re}[b(\pi_{34} + \tau_1 \pi_{13} + \bar{\tau}_2 \pi_{42} - \tau_1 \bar{\tau}_2 \pi_{12})], \quad (14)$$

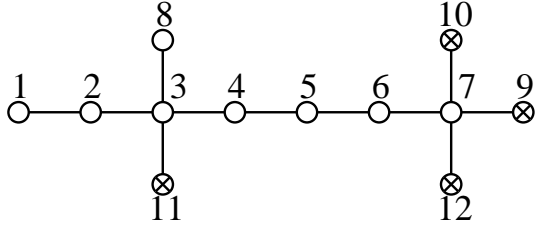


Figure 4: The Dynkin diagram of the first  $E_8$  extended by its highest root as well as the highest roots of its sublattices of types  $D_4$  and  $D_8$ .

It is well known that some  $K3$  surfaces, including  $T^4/\mathbb{Z}_2$ , allow a fixed-point free involution  $\vartheta$  yielding an Enriques surface<sup>13</sup>. The action of  $\vartheta$  on  $T^4/\mathbb{Z}_2$  is given by [23]

$$\vartheta : \quad z_1 \mapsto -z_1 + \frac{1}{2}, \quad z_2 \mapsto z_2 + \frac{1}{2}. \quad (15)$$

Hence,  $\pi_{14}$  and  $\pi_{23}$  are even under  $\vartheta$ , while  $\pi_{12}$ ,  $\pi_{34}$ ,  $\pi_{13}$  and  $\pi_{42}$  are odd. From (11) it is clear that the  $A_1$  singularities are interchanged pairwise. We will use the transformation properties of the cycles of  $T^4/\mathbb{Z}_2$  under this involution to identify them with specific cycles of the  $K3$  lattice.

We now discuss the cycles of  $T^4/\mathbb{Z}_2$  from the  $K3$  perspective. The singular limit  $T^4/\mathbb{Z}_2$  of  $K3$  is obtained by fixing the position of  $\Sigma$  such that 16 cycles with intersection matrix  $A_1^{\oplus 16}$  shrink. We start with a  $K3$  surface with an  $E_8 \times E_8$  singularity and rotate  $\Sigma$  to a  $A_1^{\oplus 16}$  point. In Sect. 2 we have specified Wilson lines breaking  $E_8$  to  $A_1^8$ . Using these Wilson lines and following the procedure detailed in Sect. 3, we will arrive at the desired point in moduli space.

We introduce a set of simple roots  $\gamma_i$ ,  $i = 1, \dots, 8, 13, \dots, 20$ , of  $\Gamma_{E_8 \times E_8}$  (cf. (1)), the highest roots  $\gamma_9$  and  $\gamma_{21}$  of the  $E_8$  root lattices as well as the highest roots  $\gamma_i$ ,  $i = 10, 11, 12, 22, 23, 24$ , of their respective sublattices of types  $D_4$  and  $D_8$  (see Fig. 4):

$$\begin{aligned} \gamma_1 &= \frac{1}{2}E_1 + \frac{1}{2}E_2 + \dots + \frac{1}{2}E_8 & \gamma_2 &= -E_7 - E_8 & \gamma_3 &= -E_6 + E_7 \\ \gamma_4 &= -E_5 + E_6 & \gamma_5 &= -E_4 + E_5 & \gamma_6 &= -E_3 + E_4 \\ \gamma_7 &= -E_2 + E_3 & \gamma_8 &= -E_7 + E_8 & \gamma_9 &= -E_1 + E_2 \\ \gamma_{10} &= E_1 + E_2 & \gamma_{11} &= E_5 + E_6 & \gamma_{12} &= -E_3 - E_4 \end{aligned}$$

---

where we defined  $\hat{a}_1 = -2a_1 \text{Im}\tau_1$  and  $\hat{a}_2 = -2a_2 \text{Im}\tau_2$ .

<sup>13</sup>Nikulin classified all involutions of  $K3$  reversing the sign of  $\omega$  [34] and found that they can be labeled by three integers  $(r, a, \delta)$ . Only one involution in this classification,  $(10, 10, 0) \equiv \vartheta$ , has no fixed points.

$$\begin{aligned}
\gamma_{13} &= \frac{1}{2}E_9 + \frac{1}{2}E_{10} + \dots + \frac{1}{2}E_{16} & \gamma_{14} &= -E_{15} - E_{16} & \gamma_{15} &= -E_{14} + E_{15} \\
\gamma_{16} &= -E_{13} + E_{14} & \gamma_{17} &= -E_{12} + E_{13} & \gamma_{18} &= -E_{11} + E_{12} \\
\gamma_{19} &= -E_{10} + E_{11} & \gamma_{20} &= -E_{15} + E_{16} & \gamma_{21} &= -E_9 + E_{10} \\
\gamma_{22} &= E_9 + E_{10} & \gamma_{23} &= E_{13} + E_{14} & \gamma_{24} &= -E_{11} - E_{12} \quad (16)
\end{aligned}$$

On the basis of (6), we choose the following Wilson-line vectors in  $\Gamma_{E_8 \times E_8}$  (The signs between the two  $E_8$  factors will be justified in a moment by the properties of the  $K3$  lattice under the Enriques involution):

$$\begin{aligned}
W^1 &= (1, 0^7, -1, 0^7), & W^2 &= (0^4, -\frac{1}{2}, 0^4, \frac{1}{2}) \\
W^3 &= (0^2, -\frac{1}{2}, \frac{1}{2}, 0^2, -\frac{1}{2}, \frac{1}{2}, 0^2, -\frac{1}{2}, \frac{1}{2}, 0^2, -\frac{1}{2}, \frac{1}{2}). \quad (17)
\end{aligned}$$

We start with  $\Sigma$  living in the  $U^{\oplus 3}$  space spanned by  $\hat{e}_1, \hat{e}^1, \hat{e}_2, \hat{e}^2, \hat{e}_3, \hat{e}^3$ . The first step is to move  $\Sigma$  in the direction of  $W^1$  by the rotation  $\hat{e}^1 \rightarrow \hat{e}^1 + W^1$ . The result is a  $K3$  surface with  $D_8 \times D_8$  singularity. While  $\gamma_1, \gamma_9, \gamma_{10}, \gamma_{13}, \gamma_{21}$  and  $\gamma_{22}$  are blown up, the cycles

$$\gamma'_9 \equiv \gamma_9 - \hat{e}_1, \quad \gamma'_{10} \equiv \gamma_{10} + \hat{e}_1, \quad \gamma'_{21} \equiv \gamma_{21} + \hat{e}_1, \quad \gamma'_{22} \equiv \gamma_{22} - \hat{e}_1 \quad (18)$$

collapse.  $\gamma'_9$  ( $\gamma'_{21}$ ) is the additional root appearing in the first (second)  $E_8$  lattice.  $\gamma'_{10}$  ( $\gamma'_{22}$ ) are the corresponding highest roots of  $D_8$ .

Next, we rotate  $\hat{e}^2 \rightarrow \hat{e}^2 + W^2$ . Since the products of  $\gamma_2, \gamma_5, \gamma_{11}, \gamma_{14}, \gamma_{17}$  and  $\gamma_{23}$  with the rotated basis vector  $\hat{e}^2 + W^2$  are all non-zero, these cycles acquire finite volume, while  $\gamma_i, i = 3, 4, 6, 7, 8, 12, 15, 16, 18, 19, 20, 24$ , and  $\gamma'_i, i = 9, 10, 21, 22$ , remain orthogonal to  $\Sigma$ . Out of the roots in (16), however, we can take those that have an integer product with  $W^2$  and construct the four further shrunk cycles

$$\gamma'_2 \equiv \gamma_2 + \hat{e}_2, \quad \gamma'_{11} \equiv \gamma_{11} - \hat{e}_2, \quad \gamma'_{14} \equiv \gamma_{14} - \hat{e}_2, \quad \gamma'_{23} \equiv \gamma_{23} + \hat{e}_2. \quad (19)$$

A set of simple roots for the orthogonal lattice  $\Lambda$  is given by  $\{\gamma_i\}_{i=3,4,6,7,8,15,16,18,19,20}$  and  $\{\gamma'_i\}_{i=2,9,10,14,21,22}$ . The intersection matrix of these simple roots is  $D_4^{\oplus 4}$ . We therefore obtained a  $K3$  surface with a  $D_4^4$  singularity.

Finally, we rotate  $\hat{e}^3 \rightarrow \hat{e}^3 + W^3$ , go to an  $A_1^{\oplus 16}$  point in  $M_{K3}$ . The roots that are

removed from  $\Lambda$  are  $\gamma_3, \gamma_6, \gamma_7, \gamma_8, \gamma_{15}, \gamma_{18}$  and  $\gamma_{19}, \gamma_{20}$ , while the new shrinking cycles are

$$\gamma'_6 \equiv \gamma_6 + \hat{e}_3, \quad \gamma'_8 \equiv \gamma_8 + \hat{e}_3, \quad \gamma'_{18} \equiv \gamma_{18} + \hat{e}_3, \quad \gamma'_{20} \equiv \gamma_{20} + \hat{e}_3. \quad (20)$$

To sum up, following the procedure outlined in the last section, we found that  $K3$  can degenerate to  $T^4/\mathbb{Z}_2$  if  $\Sigma$  is orthogonal to

$$\begin{aligned} \gamma'_2 &= -E_7 - E_8 + \hat{e}_2, & \gamma'_{14} &= -E_{15} - E_{16} - \hat{e}_2, \\ \gamma_4 &= -E_5 + E_6, & \gamma_{16} &= -E_{13} + E_{14}, \\ \gamma'_6 &= -E_3 + E_4 + \hat{e}_3, & \gamma'_{18} &= -E_{11} + E_{12} + \hat{e}_3, \\ \gamma'_8 &= -E_7 + E_8 + \hat{e}_3, & \gamma'_{20} &= -E_{15} + E_{16} + \hat{e}_3, \\ \gamma'_9 &= -E_1 + E_2 - \hat{e}_1, & \gamma'_{21} &= -E_9 + E_{10} + \hat{e}_1, \\ \gamma'_{10} &= E_1 + E_2 + \hat{e}_1, & \gamma'_{22} &= E_9 + E_{10} - \hat{e}_1, \\ \gamma'_{11} &= E_5 + E_6 - \hat{e}_2, & \gamma'_{23} &= E_{13} + E_{14} + \hat{e}_2, \\ \gamma'_{12} &= -E_3 - E_4 & \gamma'_{24} &= -E_{11} - E_{12}. \end{aligned} \quad (21)$$

This set of cycles provides a primitive embedding of the  $A_1^{\oplus 16}$  lattice into  $\Gamma_{3,19}$ .

The lattice orthogonal to the shrunk cycles  $\Upsilon$  is given by integral combinations of the following six cycles:

$$\hat{e}_1, \quad 2(\hat{e}^1 + W^1), \quad \hat{e}_2, \quad 2(\hat{e}^2 + W^2), \quad \hat{e}_3, \quad 2(\hat{e}^3 + W^3). \quad (22)$$

The 3-plane  $\Sigma$  lives in the subspace of  $H_2(K3, \mathbb{R})$  spanned by these vectors so that the cycles in  $\Upsilon$  in general have finite size. We want to identify this lattice with the  $T^4/\mathbb{Z}_2$  lattice made up of the  $\pi_{ij}$ . We will use the transformation properties of the torus-cycles  $\pi_{ij}$  under  $\vartheta$  to identify them with elements of  $\Upsilon$ .

Previously we have seen that the Enriques involution must map the singularities of  $T^4/\mathbb{Z}_2$  to each other in pairs. We hence expect that the cycles on the left column in (21) are mapped to the cycles on the right one.

Up to automorphism of  $\Gamma_{3,19}$ , the Enriques involution  $\vartheta$  acts on the  $K3$  lattice by interchanging the two  $E_8$  as well as the two  $U$ -blocks, and as  $-1$  on the remaining  $U$ -block [19] (see also [25]):

$$\vartheta : e_1 \mapsto -e_1 \quad e^1 \mapsto -e^1 \quad e_2 \leftrightarrow e_3 \quad e^2 \leftrightarrow e^3 \quad E_I \leftrightarrow E_{I+8}. \quad (23)$$

If we set  $\hat{e}_i = e_i$  and apply the transformation (23) to the 16 cycles in (21), we do not obtain what we expect, i.e. that the 8 cycles in the left column in (21) are mapped to the ones in the right column. To get this result, we need an Enriques involution such that the  $\hat{e}_i$  have definite parity. A sensible identification is thus<sup>14</sup>

$$\hat{e}_1 = e_1 \quad \hat{e}_2 = e_2 - e_3 \quad \hat{e}_3 = e^2 + e^3 \quad \hat{e}^1 = e^1 \quad \hat{e}^2 = e^2 \quad \hat{e}^3 = e_3. \quad (24)$$

Hence, the basis (22) of  $\Upsilon$  becomes

$$e_1, \quad 2(e^1 + W^1), \quad e_2 - e_3, \quad 2(e^2 + W^2), \quad e^2 + e^3, \quad 2(e_3 + W^3). \quad (25)$$

Note that the set of vectors (21) could be guessed without any reference to a particular choice of Wilson lines by going directly to the Dynkin diagram language. Then, the involution property of the three orthogonal null vectors  $\hat{e}_i$  of the  $U^{\oplus 3}$ -block that we add to rotate the shrinking cycles is determined by requiring the exchange of the two blocks.

We can now choose an integral basis of  $\Upsilon$  with the properties of  $\pi_{ij}$ , i.e. whose elements have definite parity under  $\vartheta$  and whose intersection matrix is<sup>15</sup>  $U(2)^{\oplus 3}$ :

$$\begin{array}{ll} e_1, & 2(e^1 + e_1 + W^1), \\ e_2 - e_3, & e^2 - e^3 + 2(e_2 - e_3 + W^2), \\ e^2 + e^3, & e_2 + e_3 + 2(e^2 + e^3 + W^3) \end{array} \quad (26)$$

One can check that this is an integral basis of  $\Upsilon$ . The first two lines of (26) give two  $U(2)$  blocks odd under  $\vartheta$ , while the last line gives a  $U(2)$  block even under  $\vartheta$ . Therefore, we may identify  $\pi_{23}$  and  $\pi_{14}$  with the vectors  $e^2 + e^3$  and  $e_2 + e_3 + 2(e^2 + e^3 + W^3)$  of the last  $U(2)$  block and  $\pi_{12}$ ,  $\pi_{34}$ ,  $\pi_{13}$  and  $\pi_{42}$  with the vectors  $e_1$ ,  $2(e^1 + e_1 + W^1)$ ,  $e_2 - e_3$  and  $e^2 - e^3 + 2(e_2 - e_3 + W^2)$  of the first two  $U(2)$  blocks.

## 5 $T^4/\mathbb{Z}_2$ as a double cover of $\mathbb{P}^1 \times \mathbb{P}^1$

In this section, we are going to study the connection of  $T^4/\mathbb{Z}_2$  with a smooth  $K3$  from a geometric perspective. We show how to find the lattice  $H_2(K3, \mathbb{Z})$  in a blow-up of  $T^4/\mathbb{Z}_2$ .

It is well-known that one can construct a smooth  $K3$  as a double cover [19, 22] over

---

<sup>14</sup>One can check that this transformation provides an automorphism of the lattice  $\Gamma_{3,19}$ .

<sup>15</sup>The matrix  $U(2)$  is equal to  $\begin{pmatrix} 0 & 2 \\ 2 & 0 \end{pmatrix}$ .

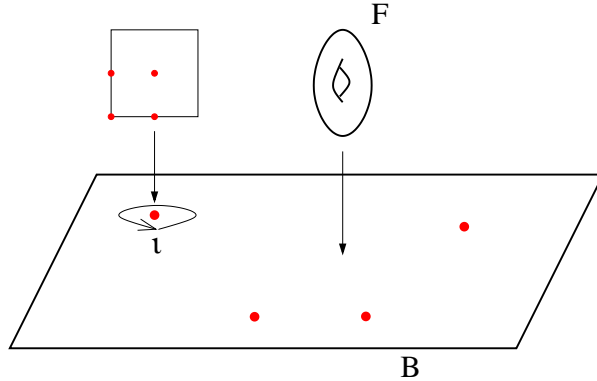


Figure 5: The elliptic fibration  $T^4/\mathbb{Z}_2 \rightarrow B = T^2/\mathbb{Z}_2$ , has four singular fibres. Upon circling one of them, the fibre torus undergoes an involution  $\iota$ . Thus any section  $B \hookrightarrow T^4/\mathbb{Z}_2$  has to pass through four singularities.

$\mathbb{P}^1 \times \mathbb{P}^1$ , branched along a curve of bidegree  $(4, 4)$ :

$$\tilde{y}^2 = h_{(4,4)}(\tilde{x}_1, \tilde{x}_2, \tilde{z}_1, \tilde{z}_2). \quad (27)$$

There are two algebraic cycles, each given by fixing a point on one of the  $\mathbb{P}^1$ s. We call the associated Divisors  $D_x$  and  $D_z$ . The corresponding curves are tori and represent the generic fibres of two different elliptic fibrations of the  $K3$  surface given by (27). As (27) gives two values of  $y$  for a generic point on  $\mathbb{P}^1 \times \mathbb{P}^1$ , we find  $D_x \cdot D_z = 2$ .

Let us choose a particular form for  $h_{(4,4)}$ :

$$y^2 = \prod_{k=1, \dots, 4} (x - x_k) \cdot (z - z_k). \quad (28)$$

For ease of exposition we have introduced the inhomogeneous coordinates  $x, y, z$ . The surface defined by (28) is easily recognized as  $T^4/\mathbb{Z}_2$ , as we explain in following: In the vicinity of the points  $(y, x, z) = (0, x_k, z_h)$ , it is given by  $y^2 = xz$ , i.e. it has sixteen  $A_1$  singularities. Let us now describe this surface as an elliptic fibration. We project to the coordinate  $x$ , so that each fibre torus is given by (28) with  $x$  fixed. The complex structure of the fibre torus is given by the ratios of the branch points  $z_k$ . As these do not depend on  $x$ , the complex structure of the fibre is constant. Over the four points in the base where  $x = x_k$ , we have  $y = 0$ , so that the fibre is  $\mathbb{P}^1$  instead of  $T^2$ , see Fig. 5. A similar fibration is obviously obtained when projecting to the  $z$ -coordinate.

This is the very same structure one finds when projecting  $T^4/\mathbb{Z}_2$  to any  $T^2/\mathbb{Z}_2$  sub-orbifold. Any of these projections can be promoted to an elliptic fibration by choosing

the complex structure of  $T^4/\mathbb{Z}_2$  appropriately. Only two of them can, however, be seen algebraically in (28). The divisors  $D_x$  and  $D_z$  correspond to multisections<sup>16</sup> (two-section) of these two fibrations. They are tori and can be identified with  $\pi_{23}$  and  $\pi_{14}$ . The other  $\pi_{ij}$  in  $T^4/\mathbb{Z}_2$  cannot be seen algebraically.

Each of the two elliptic fibrations in (28) has four proper sections. Focussing again on the fibration given by projecting to the  $x$ -coordinate, they are given by mapping  $x$  to  $(y, x, z) = (0, x, z_k)$ . Each of them passes through four  $A_1$  singularities. From the orbifold point of view, these sections are the usual divisors ( $D_{i\alpha} = \{\zeta_i = \zeta_i^{\alpha, \text{fixed}}\}$ ), given by planes lying at the fixed loci of the orbifold action [35].

We can understand how these sections arise in  $T^4/\mathbb{Z}_2$ . Fixing a projection, we have to give a point in the fibre for every point of the base in a smooth manner. As the fibre undergoes an involution when one surrounds one of the  $x_k$  in the base, the sections have to pass through one of the fixed points of this involution in the fibre. Again, not all of the sections that can be seen this way in  $T^4/\mathbb{Z}_2$  can be described algebraically in (28).

We label the sections  $\sigma_{ij}^k$  by the two directions it spans in  $T^4/\mathbb{Z}_2$  ( $i, j$ ) and the fixed point in the fibre it passes through ( $k$ ). Two  $\sigma_{ij}^k$  that span different directions in  $T^4/\mathbb{Z}_2$  are, of course, sections with respect to different elliptic fibrations. The intersection numbers with the  $\pi_{ij}$  are

$$\sigma_{ij}^k \cdot \pi_{lm} = \varepsilon_{ijklm}. \quad (29)$$

As the intersections occur away from the singularities, (29) will persist in a desingularized version of  $T^4/\mathbb{Z}_2$ .

One way to visualize the geometry of  $T^4/\mathbb{Z}_2$  is presented in Fig. 6. It will be frequently used in the rest of this paper. At present, it serves to determine which singularities are met by which  $\sigma_{ij}^k$  in the given labeling.

## 5.1 Divisors and cycles in the blow-up of $T^4/\mathbb{Z}_2$

If we blow-up the sixteen  $A_1$  singularities of  $T^4/\mathbb{Z}_2$ , we introduce sixteen exceptional divisors  $C_\lambda$  which satisfy  $C_\lambda \cdot C_\eta = -2\delta_{\lambda\eta}$ . Naively, one would guess that the lattice of integral cycles of the blow-up of  $T^4/\mathbb{Z}_2$  is thus given by  $A_1^{\oplus 16} \oplus U(2)^{\oplus 3}$ . But the blow-up of  $T^4/\mathbb{Z}_2$  should be a smooth  $K3$  surface, which has  $U^{\oplus 3} \oplus (-E_8)^{\oplus 2}$  as its lattice of integral cycles.

---

<sup>16</sup>A section is a divisor that is not part of any fibre and intersects each fibre once. Correspondingly, a multisection or  $m$ -section intersects each fibre  $m$  times.

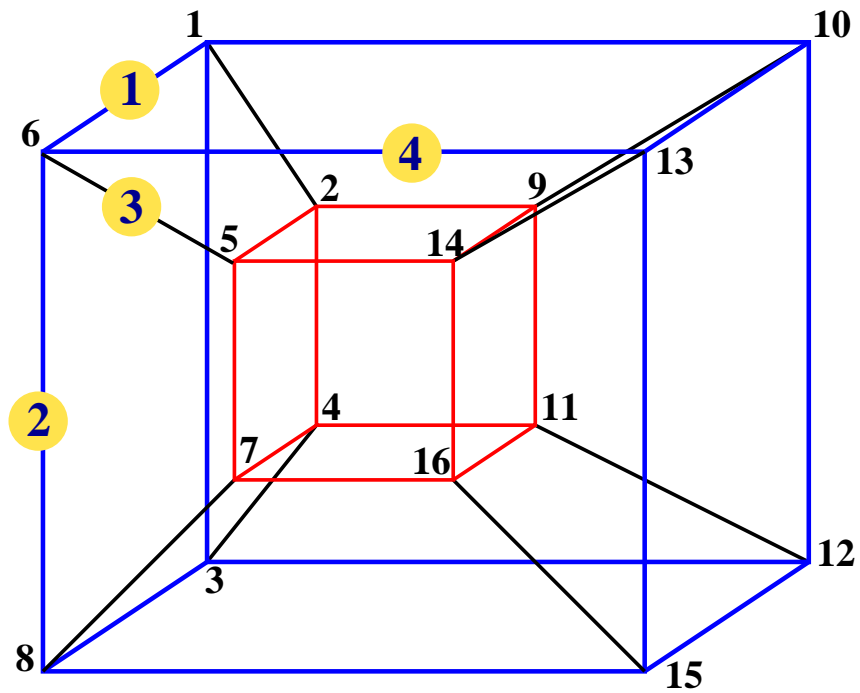


Figure 6: The set of sections  $\sigma_{ij}^k$  and the  $A_1$  singularities can be displayed as the two-dimensional faces and nodes of a four-dimensional hypercube. We picture this cube as two cubes of lower dimension whose nodes are connected as shown in the picture. We have numbered the four directions and the sixteen nodes, so that this figure can be used to determine which section meets which singularities.



The extra integral cycles are given by the preimages of the sections in the blow-up<sup>17</sup>.

To blow-up an  $A_1$  singularity (locally given by  $y^2 = xz$  in  $\mathbb{C}^3$ ) one introduces an extra  $\mathbb{P}^2$  with homogeneous coordinates  $\xi_i$  and considers the set of equations (see e.g. [36])

$$y^2 = xz, \quad \xi_1 y = x\xi_2, \quad \xi_1 z = x\xi_3, \quad \xi_2 z = y\xi_3 \quad (30)$$

in  $\mathbb{C}^3 \times \mathbb{P}^2$ . The exceptional curve  $C$  is a  $\mathbb{P}^1$  given by

$$\xi_2^2 = \xi_1 \xi_3, \quad x = y = z = 0. \quad (31)$$

Its self-intersection is  $C \cdot C = -2$ .

The sections  $\sigma$  are locally given by  $y = x = 0$ . In the blown up space  $\mathbb{C}^3 \times \mathbb{P}^2$  they are sitting at

$$x = y = 0, \quad \xi_1 = \xi_2 = 0. \quad (32)$$

This shows that the  $\sigma_{ij}^k$  lead to smooth curves in the blown-up space. We furthermore deduce that the  $\sigma$  intersect only those exceptional divisors that emerge at the four singularities they meet in  $T^4/\mathbb{Z}_2$  before the blow-up. The even cycles of  $T^4$ ,  $\pi_{ij}$ , are left completely unperturbed by the blow-up and cannot intersect any of the exceptional divisors. We thus find the following intersections in the smooth  $K3$ :

$$C_\lambda \cdot C_\eta = -2\delta_{\lambda\eta}, \quad \pi_{ij} \cdot \pi_{ml} = 2\varepsilon_{ijml}, \quad C_\lambda \cdot \pi_{ij} = 0, \quad (33)$$

$$\sigma_{ij}^k \cdot \pi_{ml} = \varepsilon_{ijml}, \quad \sigma_{jl}^k \cdot C_\lambda = 1 \text{ if } i \in I_{jl}^k, \quad \sigma_{jl}^k \cdot C_\lambda = 0 \text{ if } i \notin I_{jl}^k. \quad (34)$$

The index sets  $I_{jl}^k$  can e.g. be determined from Fig. 6 (remember that the  $\sigma_{jl}^k$  correspond to the faces of the hypercube). As we know that the second homology of  $K3$  is 22-dimensional and the cycles  $C_\lambda$  and  $\pi_{ml}$  are independent, it is clear that we can use them as a basis for  $H_2(K3, \mathbb{R})$ . Thus there exists an expansion of the cycles  $\sigma_{jl}^k$  in terms of this

---

<sup>17</sup>Remember that a blow-up actually is a projection mapping the blown-up space to the space one starts with [36].

basis. Using the intersection numbers (34), we conclude that<sup>18</sup>

$$\sigma_{ij}^k = \frac{1}{2} \cdot (\pi_{ij} - \sum_{\lambda \in I_{ji}^k} C_\lambda). \quad (35)$$

Before, we have shown that the  $\sigma_{ij}^k$  are in fact elements of the *integral* homology of the smooth, blown-up  $K3$ . On the other hand we see from (35) that they are not integral combinations of the  $\pi_{ij}$  and  $C_\lambda$ . This tells us that the lattice of integral cycles consists of many more elements than the ones in  $A_1^{\oplus 16} \oplus U(2)^{\oplus 3}$ : it must also contain all elements of the form (35). It can moreover be shown that out of the  $\sigma_{ij}^k$  and  $C_\lambda$  one can construct a basis of integral cycles that has an intersection matrix with determinant minus one. As all self-intersections are even numbers, we have thus constructed an even unimodular lattice of signature (3, 19). This lattice must be  $\Gamma_{3,19} = U^{\oplus 3} \oplus (-E_8)^{\oplus 2}$ , the lattice of integral cycles of  $K3$  [27].

Note that the symmetries of  $T^4/\mathbb{Z}_2$  are manifest in our construction. They simply correspond to a relabeling of or a reflection along one of the four directions of the cube in Fig. 6.

A similar construction of  $\Gamma_{3,19} = H_2(K3, \mathbb{Z})$  has recently been discussed in [37]. There it is exploited that  $H_2(K3, \mathbb{Z})$  must be an unimodular lattice. This property of  $H_2(K3, \mathbb{Z})$  is used to systematically enlarge  $U(2)^{\oplus 3} \oplus A_1^{\oplus 16}$  to  $\Gamma_{3,19}$ . Our presentation differs in that we *geometrically* identify the elements  $\sigma_{ij}^k$  that enlarge the lattice  $U(2)^{\oplus 3} \oplus A_1^{\oplus 16}$  to  $\Gamma_{3,19}$ .

Related discussions of how to find integral cycles after blowing up singularities appear in [35] in the context of type IIB compactifications and in [11] in the context of heterotic orbifolds (see also [12–15]).

## 5.2 Juxtaposition

In the first part of this section, we have given a detailed description of the six finite size cycles of  $T^4/\mathbb{Z}_2$  and of its collapsed cycles. We have then identified them with holomorphic cycles in an algebraic model. Using the results of Sect. 4, we are able to match these cycles

---

<sup>18</sup> This expression is consistent with those of the intersections between the  $\sigma_{ij}^k$  that can be checked algebraically: If two faces do not meet at all, their intersection number is clearly zero both algebraically and by (35). If they have one node in common, their intersection number is still zero from (35). This agrees with the algebraic model where one can check that these two cycles miss each other in the blown-up  $K3$ . If two sections have two nodes in common, they can not be represented by algebraic subvarieties of (28). In this situation (35) determines their mutual intersection to be unity.

with the conventionally labelled  $K3$  lattice of Sect. 3 <sup>19</sup>:

The six torus cycles  $\pi_{ij}$  are:

$$\begin{aligned}
\pi_{23} &= e^2 + e^3 & \pi_{14} &= e_2 + e_3 + 2(e^2 + e^3) + 2W^3 \\
\pi_{12} &= e_1 & \pi_{34} &= 2(e^1 + e_1) + 2W^1 \\
\pi_{13} &= e_2 - e_3 & \pi_{42} &= e^2 - e^3 + 2(e_2 - e_3) + 2W^2, \tag{36}
\end{aligned}$$

with  $W^1, W^2, W^3$  given in (17).

The exceptional cycles  $C_\lambda$  are identified with the cycles in (21):

$$\begin{aligned}
C_1 &= E_1 + E_2 + e_1 & C_9 &= E_9 + E_{10} - e_1 \\
C_2 &= -E_1 + E_2 - e_1 & C_{10} &= -E_9 + E_{10} + e_1 \\
C_3 &= -E_3 - E_4 & C_{11} &= -E_{11} - E_{12} \\
C_4 &= -E_3 + E_4 + e^2 + e^3 & C_{12} &= -E_{11} + E_{12} + e^2 + e^3 \\
C_5 &= -E_5 + E_6 & C_{13} &= -E_{13} + E_{14} \\
C_6 &= E_5 + E_6 - e_2 + e_3 & C_{14} &= E_{13} + E_{14} + e_2 - e_3 \\
C_7 &= -E_7 + E_8 + e^2 + e^3 & C_{15} &= -E_{15} + E_{16} + e^2 + e^3 \\
C_8 &= -E_7 - E_8 + e_2 - e_3 & C_{16} &= -E_{15} - E_{16} - e_2 + e_3. \tag{37}
\end{aligned}$$

A non-trivial check of the identifications made above is to use (9) to show that all of the  $\sigma_{ij}^k$  as given in (35) are indeed elements of the  $K3$  lattice. The results are collected in the appendix.

We can now easily write down the roots of  $E_8 \times E_8$  and the basis vectors  $e_i, e^i$  of the three hyperbolic lattices in terms of the integral cycles we have found in the blow-up. In terms of the standard labeling, they are given by

$$\begin{aligned}
1 : \frac{1}{2} \sum_{i=1}^8 E_i &= -\sigma_{12}^1 - C_3 - C_8 + \pi_{13} & 2 : -E_7 - E_8 &= C_8 - \pi_{13} \\
3 : -E_6 + E_7 &= \sigma_{23}^1 & 4 : -E_5 + E_6 &= C_5 \\
5 : -E_4 + E_5 &= \sigma_{13}^1 - \sigma_{23}^2 + \pi_{23} + C_6 - C_4 & 6 : -E_3 + E_4 &= C_4 - \pi_{23} \\
7 : -E_2 + E_3 &= \sigma_{23}^2 & 8 : -E_7 + E_8 &= C_7 - \pi_{23} \tag{38}
\end{aligned}$$

---

<sup>19</sup> This shows that the embedding of  $A_1^{\oplus 16} \subset H_2(K3, \mathbb{Z})$  obtained in the first half of this paper is identical with the embedding of the  $C_\lambda$  that is implicit from the last section.

for the first  $E_8$  and by

$$\begin{aligned}
1 : \frac{1}{2} \sum_{i=9}^{16} E_i &= -\sigma_{12}^3 - C_{16} - C_{11} + \pi_{12} - \pi_{13} & 2 : -E_{15} - E_{16} &= C_{16} + \pi_{13} \\
3 : -E_{14} + E_{15} &= \sigma_{23}^4 & 4 : -E_{13} + E_{14} &= C_{13} \\
5 : -E_{12} + E_{13} &= \sigma_{13}^2 - \pi_{13} - \sigma_{23}^3 + \pi_{23} + C_{14} - C_{12} & 6 : -E_{11} + E_{12} &= C_{12} - \pi_{23} \\
7 : -E_{10} + E_{11} &= \sigma_{23}^3 & 8 : -E_{15} + E_{16} &= C_{15} - \pi_{23}
\end{aligned} \tag{39}$$

for the second  $E_8$ . We furthermore find that

$$\begin{aligned}
e_1 &= \pi_{12} & e^1 &= \sigma_{34}^2 + C_2 + C_9 + \pi_{12} \\
e_2 &= \pi_{13} + e_3 & e^2 &= \pi_{23} - e^3 \\
e_3 &= \sigma_{14}^1 - C_7 - C_4 - \sigma_{13}^4 + \pi_{23} & e^3 &= \sigma_{42}^2 - C_{16} + C_8 + \sigma_{23}^1 - \pi_{13} .
\end{aligned} \tag{40}$$

## 6 The Enriques involution

In this section we will describe the Enriques involution in detail.

Let us first determine its action on the sixteen  $A_1$  singularities and the corresponding exceptional divisors from its action on  $H_2(K3, \mathbb{Z})$  [19, 25]:

$$\vartheta : e_1 \mapsto -e_1 \quad e^1 \mapsto -e^1 \quad e_2 \leftrightarrow e_3 \quad e^2 \leftrightarrow e^3 \quad E_I \leftrightarrow E_{I+8} . \tag{41}$$

From (37) we see that  $C_\lambda \leftrightarrow C_{\lambda+8}$ . Considering Fig. 6, this means that the singularities are exchanged along the 3-4-directions. This can be reproduced from the action of the Enriques involution on  $T^4/\mathbb{Z}_2$ , see (15). We can also see the same behavior in the description of  $T^4/\mathbb{Z}_2$  as a hypersurface, (28): By shifting and rescaling  $x$  and  $z$ , we can always arrange that  $x_1 = -x_2$ ,  $x_3 = -x_4$  and  $z_1 = -z_2$ ,  $z_3 = -z_4$ . The Enriques involution then acts as  $\vartheta : (y, x, z) \mapsto (-y, -x, -z)$  [19], so that the sixteen  $A_1$  singularities are exchanged as noted before.

To fix an elliptic fibration of  $T^4/\mathbb{Z}_2$ , we first select  $\pi_{23} = e^2 + e^3$  as the homology class of the generic fibre. It is obviously invariant under the Enriques involution (41). The sections are then given by the  $\sigma_{14}^k$ , see Figs. 6 and 7. They can be expressed in terms of the  $K3$

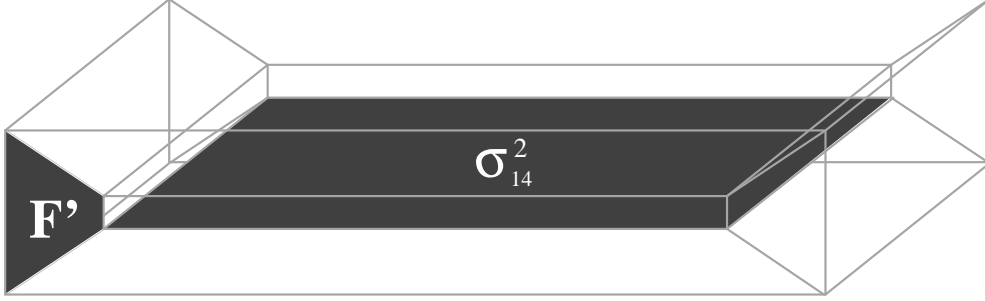


Figure 7: Choosing the generic fibre to be in the homology class  $\pi_{23}$ , the sections are in the 1-4 direction (compare with Fig. 6). We have depicted the section  $\sigma_{14}^2$  and the finite-size component of one of the singular fibres,  $F' = \sigma_{23}^1$ .

lattice as

$$\begin{aligned}
\sigma_{14}^1 &= e_3 + E_4 + E_8 \\
\sigma_{14}^2 &= e_2 + E_{12} + E_{16} \\
\sigma_{14}^3 &= e_1 + e_3 + e^2 + e^3 + \frac{1}{2}(E_1 - E_2 - E_3 + E_4 + E_5 - E_6 - E_7 + E_8) \\
&\quad + \frac{1}{2}(-E_9 - E_{10} - E_{11} + E_{12} - E_{13} - E_{14} - E_{15} + E_{16}) \\
\sigma_{14}^4 &= -e_1 + e_2 + e^3 + e^2 + \frac{1}{2}(-E_1 - E_2 - E_3 + E_4 - E_5 - E_6 - E_7 + E_8) \\
&\quad + \frac{1}{2}(E_9 - E_{10} - E_{11} + E_{12} + E_{13} - E_{14} - E_{15} + E_{16}). \tag{42}
\end{aligned}$$

The Enriques involution acts by exchanging them pairwise. This implies that the resulting Enriques surface is elliptically fibred with a two-section, i.e.  $\tilde{B} \cdot \tilde{F} = 2$ . This result is expected from the general theory of Enriques surfaces [19]. Note that the pairwise exchange of the sections under the Enriques involution can also be seen from (28).

## 6.1 The standard Weierstrass model

We now want to make contact with a Weierstrass model with constant  $\tau$ . It takes the form [38]

$$y^2 = x^3 + \alpha_1 h^2 x z^4 + \alpha_2 h^3 z^6 = (x - \gamma_1 z^2 h)(x - \gamma_2 z^2 h)(x - \gamma_3 z^2 h). \tag{43}$$

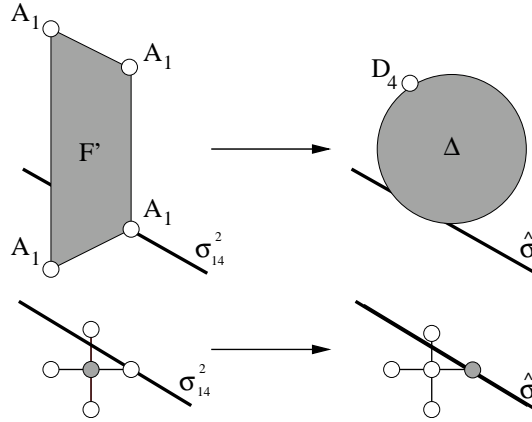


Figure 8: When blowing up the  $A_1$  singularity hit by the section  $\sigma_{14}^2$  while collapsing the  $F'$  component of the singular fibre, we produce a  $D_4$  singularity. This  $D_4$  singularity is not hit by the section  $\sigma_{14}^2$ , which is then identified with  $\hat{\sigma}$ . In this figure we display singularities and collapsed cycles in white and cycles of finite size in light grey. In the lower part of the figure we have drawn the intersection pattern between the cycles in a diagrammatic fashion. After the  $F'$  component of the singular fibre is blown down and the  $A_1$  singularity hit by the section is blown up, the collapsed cycles intersect according to the Dynkin diagram of  $SO(8)$ , so that this operation produces a  $D_4$  singularity.

Here  $\gamma_i$  and  $\alpha_i$  are complex constants and  $h$  is a homogeneous polynomial of the base coordinates of degree 4. Contrary to  $T^4/\mathbb{Z}_2$ , the surface described by this equation has four  $D_4$  singularities. There are three sections given by  $y = 0, x = \gamma_i z^2 h$  that pass through the four  $D_4$  singularities at  $y = x = h = 0$ . The fourth section at  $x^3 = y^2, z = 0$  does not hit any singularity. This section is a special feature of the Weierstrass model and we will denote it by  $\hat{\sigma}$  in the following.

From what we have said, it is clear that  $T^4/\mathbb{Z}_2$  cannot be described by a Weierstrass model. In fact, the section  $\hat{\sigma}$  must be orthogonal to all shrinking cycles, and then, for  $T^4/\mathbb{Z}_2$  it should belong to  $\Upsilon$  (see (26)). But this is not possible, since this is a lattice with all intersection numbers being even, and the section  $\hat{\sigma}$  should have intersection one with the fibre.

Intuitively, there is an obvious way how to get from  $T^4/\mathbb{Z}_2$  to an elliptic  $K3$  described by (43). First, we choose one of the sections of  $T^4/\mathbb{Z}_2$ , say  $\sigma_{14}^2$ , that is to become  $\hat{\sigma}$ . We then blow up the singularities which are hit by this section while blowing down the finite-size components  $F'$  of the four singular fibres. We have depicted this deformation in Fig. 8. The section  $\sigma_{14}^2$ , which is now identified with  $\hat{\sigma}$ , no longer intersects any singularities and the lattice of collapsed cycles is exactly  $D_4^{\oplus 4}$ . The other three sections are all forced to meet



To specify a complex structure compatible with the Enriques involution, we have to choose  $\omega$  as a linear combination of the odd cycles in (44) and  $j$  as a linear combination of the even cycles in (44). As  $\pi_{23}$  is the only even cycle,  $j$  must be proportional to it. This, however, violates the requirement  $j \cdot j > 0$ .

We can also see the clash between the Weierstrass model description and the Enriques involution from a different perspective. We start with the 3-plane  $\Sigma$  in the lattice  $\Upsilon$  (see (26)). Since we want a complex structure compatible with a holomorphic Enriques involution, we take  $\omega$  in the odd subspace of  $\Upsilon$ . We now try to make the rotation to an  $SO(8)^4$  point, maintaining the symmetry under the Enriques involution. Since the third Wilson line  $W^3$  is symmetric under the Enriques involution, we can switch it off without destroying the symmetry. Note that this means that we have only changed  $j$ . From the discussion of Sect. 2 to Sect. 4 it is clear that removing  $W^3$  will result in a  $K3$  with four  $D_4$  singularities. Now the 3-plane  $\Sigma$  lives in<sup>21</sup>

$$\begin{aligned} \pi_{23} &= e^2 + e^3, & e_2 + e_3, \\ \pi_{12} &= e_1, & \pi_{34} = 2(e^1 + e_1 + W^1), \\ \pi_{13} &= e_2 - e_3, & \pi_{42} = e^2 - e^3 + 2(e_2 - e_3 + W^2). \end{aligned} \tag{46}$$

Comparing with (44), we see that we have replaced  $\sigma_{14}^2$  by  $e_2 + e_3$ . This means that this time we have blown up the cycles  $C_4, C_7, C_{12}, C_{15}$  while shrinking the cycles  $\sigma_{23}^k$ . When  $\Sigma$  lives in (46), we can find a section that does not meet any singularities, e.g.  $e_2 - (e^2 + e^3)$ . However, there exists no choice for  $\omega$  such that  $\omega$  is odd and orthogonal to this section at the same time. In fact, these two conditions require  $\omega$  to live in a subspace with degenerate metric, as can be seen by looking back at (46). The complex structure that is demanded by the holomorphicity of the section  $\hat{\sigma}$  and the complex structure demanded by the Enriques involution are not compatible.

In summary: Starting from  $T^4/\mathbb{Z}_2$ , there are two ways to rotate the 3-plane  $\Sigma$  such as to get a Weierstrass model with  $D_4^{\oplus 4}$  singularity. They have different behavior with respect to the Enriques involution: In the first case, we destroy the symmetry. In the second case, the symmetry is preserved, but there is no choice of complex structure that both admits a holomorphic section (which does not hit the singularities) and makes the Enriques involution holomorphic.

---

<sup>21</sup>Notice that, in contrast to (44), these cycles do not generate the lattice orthogonal to the shrinking cycles.



## 6.2 A symmetric Weierstrass model

In the standard Weierstrass model description, in which the fibre is embedded as a hypersurface in  $\mathbb{P}_{1,2,3}$ , one always has one section  $\hat{\sigma}$ . By embedding the fibre in other spaces, it is possible to obtain elliptic  $K3$  surfaces with two or more sections [24, 25]. In particular, it is known that embedding the fibre in  $\mathbb{P}_{1,1,2}$  yields an elliptic  $K3$  with two sections which are permuted under the Enriques involution [25]. This elliptic  $K3$  is given by an equation of the form

$$y^2 = x^4 + x^2 z^2 f_4 + z^4 f_8. \quad (47)$$

The  $\mathbb{Z}_2$  transformation  $(y, x, z) \mapsto (-y, x, -z)$  together with a holomorphic involution of the  $\mathbb{P}^1$  base has no fixed points and projects out the holomorphic two-form, so that it provides an Enriques involution of  $K3$ . The two holomorphic sections  $\hat{\sigma}_1, \hat{\sigma}_2$  are given by  $z = 0, y = \pm x^2$  and are permuted under the Enriques involution. The  $j$ -function of this fibration is given by [25]:

$$\frac{1}{108} \frac{(f_4^2 + 12f_8)^3}{f_8(-f_4^2 + 4f_8)^2}. \quad (48)$$

Let us discuss the limit in which the complex structure of the fibre is constant. To achieve this, we take  $f_8 = f_4^2$ . Setting  $z = 1$  and shifting  $f_4$  by some multiple of  $x^2$  to complete the square<sup>22</sup>, we find the equation

$$y^2 = f_4'^2 + x^4. \quad (49)$$

Thus there are four  $A_3$  singularities at the four points  $f_4 = x = y = 0$ .

Let us find this configuration by deforming  $T^4/\mathbb{Z}_2$ . The strategy is similar to that employed for the deformation of  $T^4/\mathbb{Z}_2$  to a  $D_4^{\oplus 4}$  configuration. In order to get two sections that do not hit any singularities and that are interchanged by the Enriques involution we have to blow up  $C_\lambda$ ,  $\lambda = 3, 4, 7, 8, 11, 12, 15, 16$ . At the same time we shrink the cycles  $\sigma_{23}^k$  to produce four  $A_3$  singularities, see Fig. 9.

This can be realized by<sup>23</sup>

$$\begin{aligned} j &= b\pi_{23} + f\pi_{14} - \frac{f}{2} \sum_{\lambda} C_{\lambda} = b\pi_{23} + f(\sigma_{14}^1 + \sigma_{14}^2), \\ \omega &= \pi_{34} + U\pi_{13} + S\pi_{42} - US\pi_{12}. \end{aligned} \quad (50)$$

---

<sup>22</sup>Note that this is a bijective map between the coordinates  $y, x, f_4$  and  $y, x, f_4'$ .

<sup>23</sup>We have chosen  $j$  and  $\omega$  in a six-dimensional subspace of the 10-dimensional space orthogonal to the 12  $A_3^{\oplus 4}$  cycles. The lattice of cycles orthogonal to a generic  $\Sigma$ , i.e. orthogonal to the six basis cycles of (50), then has a dimension which is bigger than 12. By examining this lattice, one can check that in spite of this the singularity is still  $A_3^{\oplus 4}$ . Another way to see this is through the associated Wilson-line breaking.

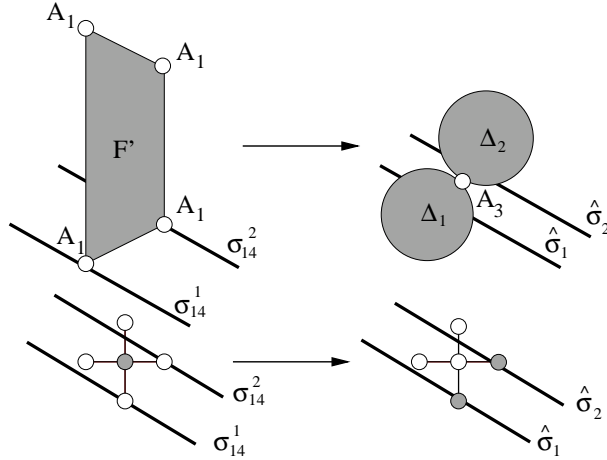


Figure 9: When blowing up two  $A_1$  singularities while shrinking the finite-size component of the singular fibre, we produce an  $A_3$  singularity and two sections,  $\hat{\sigma}_1$  and  $\hat{\sigma}_2$ , which do not hit any singularities. This works in a similar way as the deformation of  $T^4/\mathbb{Z}_2$  to an  $SO(8)^{\oplus 4}$  configuration, see Fig. 8. We again display singularities and collapsed cycles in white and cycles of finite size in light grey.

Here  $f$  gives the volume of the elliptic fibre. The two sections  $\hat{\sigma}_1 = \sigma_{14}^1$  and  $\hat{\sigma}_2 = \sigma_{14}^2$  are orthogonal to  $\omega$  and do not intersect any of the collapsed cycles.  $j$  and  $\omega$  have the right transformation properties under the Enriques involution.

## 7 F-theory Limit

There is more than one way to construct an elliptic Calabi-Yau  $(n+1)$ -fold that describes a type IIB orientifold compactification on a Calabi-Yau  $n$ -fold  $CY_n$  with D7-charge cancelled locally<sup>24</sup>. The examples we discuss here fall into two classes:

1. Weierstrass models with constant  $\tau$ .
2. Fourfolds  $(CY_n \times T^2)/\mathbb{Z}_2$ , where the  $\mathbb{Z}_2$  acts as an orientifold involution on  $CY_n$  and inverts the complex coordinate  $z$  of  $T^2$ , see e.g [42].

The corresponding M-theory backgrounds are different. It is only in the F-theory limit that they are dual to the same type IIB background. We will illustrate this fact for the simple examples described in this paper and consider an elliptically fibred Calabi-Yau two-fold,

<sup>24</sup>Running Sen's weak coupling limit [38,40,41] backwards, a general procedure to construct an F-theory Calabi-Yau 4-fold, given a generic type IIB setup with D7-branes and O7/O3-planes, was obtained in [9,10].

i.e.  $K3$ , whose fibre has a constant complex structure. We consider two different types of Weierstrass models with constant  $\tau$  and the  $T^4/\mathbb{Z}_2$  limit of  $K3$ :

- *An elliptically fibred  $K3$  with one distinguished section.* There are four points on the base  $\mathbb{P}^1$  where the 2-fold develops a  $D_4$  singularity. The cycles corresponding to fibre and section are  $F = \pi_{23}$  and  $\hat{\sigma} = \sigma_{14}^2$ . The Kähler form and the complex structure live in the space (44). They can be chosen as<sup>25</sup>:

$$\begin{aligned} j &= b \pi_{23} + f \sigma_{14}^2, \\ \omega &= \pi_{34} + U \pi_{13} + S \pi_{42} - U S \pi_{12}. \end{aligned} \tag{51}$$

This point in moduli space is the one reached from  $T^4/\mathbb{Z}_2$  by the rotation of  $j$  described in Sect. 6.1.

- *An elliptically fibred  $K3$  with two distinguished sections.* Again there are four points on the base where the two-fold develops a singularity. This time, however, this is an  $A_3$  singularity, as described in Sect. 6.2. The Kähler form and the complex structure can be given by

$$\begin{aligned} j &= b \pi_{23} + f (\sigma_{14}^1 + \sigma_{14}^2), \\ \omega &= \pi_{34} + U \pi_{13} + S \pi_{42} - U S \pi_{12}. \end{aligned} \tag{52}$$

- *The space  $(T^2 \times T^2)/\mathbb{Z}_2$ , i.e. the  $T^4/\mathbb{Z}_2$  limit of  $K3$ .* This manifold has 16  $A_1$  singularities. One choice for the Kähler form and the complex structure is

$$\begin{aligned} j &= b \pi_{23} + f \pi_{14}, \\ \omega &= \pi_{34} + U \pi_{13} + S \pi_{42} - U S \pi_{12}. \end{aligned} \tag{53}$$

We notice that the only difference between the three cases is the expression for the Kähler form  $j$ .

Compactifying M-theory on these manifolds gives different 7-dimensional spectra, as all three have different singularities. In particular, we obtain the gauge groups  $SO(8)^4$  in the first case,  $SO(6)^4 \times U(1)^4$  in the second case and  $SU(2)^{16}$  in the third case. In the

---

<sup>25</sup>The most general expression for  $j$  also includes two deformations in  $\langle \pi_{12}, \pi_{34}, \pi_{13}, \pi_{42} \rangle$ ; we do not include these here, as they are not relevant for the 7-dimensional gauge group and go to zero in the F-theory limit [43, 44].

dual type IIB model on  $S_B^1 \times T^2/\mathbb{Z}_2$ , we have four D7-branes on top of each O7-plane wrapping  $S_B^1$ . However, in the second and third case the gauge group is broken by Wilson lines along the  $S_B^1$ <sup>26</sup>. On the type IIB side, the F-theory limit is given by  $R_B \rightarrow \infty$ . In this limit the  $S_B^1$  decompactifies and the Wilson lines become trivial, leaving  $SO(8)^4$  as the 8-dimensional gauge group.

Let us have a more detailed look at the F-theory limit from the M-theory perspective, i.e., we send the fibre size to zero and see how the Kähler form and the complex structure behave.

- In the first case the F-theory limit is described in [43]: since the fibre  $F$  is orthogonal to  $\omega$ , its size is given by

$$\rho(F) = \int_F j = F \cdot j = f. \quad (54)$$

This vanishes in the F-theory limit  $f \rightarrow 0$ , and the Kähler form becomes  $j \rightarrow b \pi_{23}$ .

Note that we find some further shrinking cycles in this limit:  $C_4, C_7, C_{11}, C_{16}$  only have a finite size due to their intersection with  $\sigma_{14}^2$  in  $j$ . Letting  $f \rightarrow 0$  they collapse so that the intersection pattern of shrunk cycles is now four times the *extended* Dynkin diagram of  $SO(8)$ . This is expected from a general perspective: The component of the fibre that has finite size and the four associated collapsed cycles have the extended Dynkin diagram of  $SO(8)$  as their intersection pattern (see Fig. 8). Their sum, i.e the singular fibre, is homologous to the generic fibre, see e.g. (35). Sending the volume of the generic fibre to zero, all five cycles have to collapse.

- The second case differs only through the term proportional to  $f$  in the Kähler form  $j$ . In the limit  $f \rightarrow 0$  we thus reach the same point in the moduli space of  $K3$ .
- The same happens for  $T^4/\mathbb{Z}_2$ . Our choice of  $j$  and  $\omega$  has of course been completely arbitrary. Using Fig. 6, we can easily discuss the most general case:  $j$  is then given as

$$j = f \pi_{ij} + b \pi_{ml}, \quad (55)$$

with four different indices  $i, j, m, l$ . The holomorphic two-form  $\omega$  lives in the space spanned by the  $\pi_{pq}$  that have zero intersection with the Kähler form (55). Besides the sixteen cycles  $C_\lambda$  we find that all of the four  $\sigma_{ml}^k$  (with  $k = 1, \dots, 4$ ) are collapsed

---

<sup>26</sup>The deformations of  $j$  inside the  $SO(8)$  cycles are mapped to the 8th component of the type IIB vectors (see [44] for details).

when  $f \rightarrow 0$ . These 20 cycles intersect precisely according to the extended Dynkin diagram of  $SO(8)^{\oplus 4}$ , as expected.

We have found a geometric realization of the result in [43]: deforming  $j$  does not alter the point in moduli space reached in the F-theory limit: It sets to zero all components of  $j$  except the fibre. If we have multiple sections, they collapse to a single one in the F-theory limit.

We also found an important result: Before the F-theory limit, the Enriques involution is consistent only with  $T^4/\mathbb{Z}_2$  and the symmetric Weierstrass model. *In the F-theory limit the Enriques involution is also consistent with the standard Weierstrass model.*

## 8 Conclusions and Outlook

In this note we have obtained an explicit embedding of the lattice of cycles that are collapsed when  $K3$  degenerates to  $T^4/\mathbb{Z}_2$  in  $H_2(K3, \mathbb{Z})$ . This embedding leads to a highly symmetric representation of  $H_2(K3, \mathbb{Z})$ .

We have shown geometrically that  $T^4/\mathbb{Z}_2$  and the two Weierstrass-model  $K3$ s discussed in this paper are equivalent in the F-theory limit. Away from that limit, their crucial difference lies in the structure of their sections. In the case of an elliptic  $K3$  described by a standard Weierstrass model, the presence of the distinguished section  $\hat{\sigma}$  is inconsistent with the Enriques involution (except in the F-theory limit).

As an application of our detailed description of the Enriques involution we envisage the generalization of the flux-stabilization analyses on  $K3 \times K3$  [43, 45–48] to  $(K3 \times K3)/\mathbb{Z}_2^E$ . Here we assume that  $\mathbb{Z}_2^E$  acts as an Enriques involution on one  $K3$  and as a generic holomorphic (not necessarily fixed-point-free) involution on the other  $K3$ . As we have shown, we cannot use the standard Weierstrass model description for  $K3$  as long as we are not in F-theory limit. Our results show that this does not represent a problem: as long as we make sure that  $\omega \rightarrow -\omega$  under the Enriques involution,  $j$  will become symmetric in the F-theory limit. Furthermore, in this limit the standard Weierstrass model description is equivalent to other descriptions which stay symmetric also for finite fibre volume.

## Acknowledgments

We would like to thank Bobby Acharya, Francesco Benini, Mboyo Esole, Barbara Fantechi, Stefan Groot Nibbelink, Christoph Lüdeling and Michele Trapletti for useful discussions.

## A Explicit expressions for the $\sigma_{ij}^k$

$$\begin{aligned}
\sigma_{14}^1 &= \frac{1}{2} (\pi_{14} - C_3 - C_8 - C_{12} - C_{15}) = e_3 + E_4 + E_8 \\
\sigma_{14}^2 &= \frac{1}{2} (\pi_{14} - C_4 - C_7 - C_{11} - C_{16}) = e_2 + E_{12} + E_{16} \\
\sigma_{14}^3 &= \frac{1}{2} (\pi_{14} - C_2 - C_5 - C_9 - C_{14}) = e_1 + e_3 + e^2 + e^3 \\
&\quad + \frac{1}{2} (E_1 - E_2 - E_3 + E_4 + E_5 - E_6 - E_7 + E_8) \\
&\quad + \frac{1}{2} (-E_9 - E_{10} - E_{11} + E_{12} - E_{13} - E_{14} - E_{15} + E_{16}) \\
\sigma_{14}^4 &= \frac{1}{2} (\pi_{14} - C_1 - C_6 - C_{10} - C_{13}) = -e_1 + e_2 + e^3 + e^2 \\
&\quad + \frac{1}{2} (-E_1 - E_2 - E_3 + E_4 - E_5 - E_6 - E_7 + E_8) \\
&\quad + \frac{1}{2} (E_9 - E_{10} - E_{11} + E_{12} + E_{13} - E_{14} - E_{15} + E_{16}). \tag{56}
\end{aligned}$$

$$\begin{aligned}
\sigma_{23}^1 &= \frac{1}{2} (\pi_{23} - C_5 - C_6 - C_7 - C_8) = E_7 - E_6 \\
\sigma_{23}^2 &= \frac{1}{2} (\pi_{23} - C_1 - C_2 - C_3 - C_4) = E_3 - E_2 \\
\sigma_{23}^3 &= \frac{1}{2} (\pi_{23} - C_9 - C_{10} - C_{11} - C_{12}) = E_{11} - E_{10} \\
\sigma_{23}^4 &= \frac{1}{2} (\pi_{23} - C_{13} - C_{14} - C_{15} - C_{16}) = E_{15} - E_{14} \tag{57}
\end{aligned}$$

$$\begin{aligned}
\sigma_{12}^1 &= \frac{1}{2} (\pi_{12} - C_1 - C_3 - C_6 - C_8) \\
&= \frac{1}{2} (-E_1 - E_2 + E_3 + E_4 - E_5 - E_6 + E_7 + E_8) \\
\sigma_{12}^2 &= \frac{1}{2} (\pi_{12} - C_2 - C_4 - C_5 - C_7) \\
&= e_1 - e^2 - e^3 + \frac{1}{2} (E_1 - E_2 + E_3 - E_4 + E_5 - E_6 + E_7 - E_8) \\
\sigma_{12}^3 &= \frac{1}{2} (\pi_{12} - C_9 - C_{11} - C_{14} - C_{16}) \\
&= e_1 + \frac{1}{2} (-E_9 - E_{10} + E_{11} + E_{12} - E_{13} - E_{14} + E_{15} + E_{16}) \\
\sigma_{12}^4 &= \frac{1}{2} (\pi_{12} - C_{10} - C_{12} - C_{13} - C_{15}) \\
&= -e^2 - e^3 + \frac{1}{2} (E_9 - E_{10} + E_{11} - E_{12} + E_{13} - E_{14} + E_{15} - E_{16}) \tag{58}
\end{aligned}$$

$$\begin{aligned}
\sigma_{34}^1 &= \frac{1}{2}(\pi_{34} - C_5 - C_6 - C_{13} - C_{14}) = e_1 + e^1 + E_1 - E_6 - E_9 - E_{14} \\
\sigma_{34}^2 &= \frac{1}{2}(\pi_{34} - C_1 - C_2 - C_9 - C_{10}) = e_1 + e^1 + E_1 - E_2 - E_9 - E_{10} \\
\sigma_{34}^3 &= \frac{1}{2}(\pi_{34} - C_3 - C_4 - C_{11} - C_{12}) = e_1 + e^1 - e^2 - e^3 + E_1 + E_3 - E_9 + E_{11} \\
\sigma_{34}^4 &= \frac{1}{2}(\pi_{34} - C_7 - C_8 - C_{15} - C_{16}) = e_1 + e^1 - e^2 - e^3 + E_1 + E_7 - E_9 + E_{15} \quad (59)
\end{aligned}$$

$$\begin{aligned}
\sigma_{13}^1 &= \frac{1}{2}(\pi_{13} - C_1 - C_2 - C_5 - C_6) = e_2 - e_3 - E_2 - E_6 \\
\sigma_{13}^2 &= \frac{1}{2}(\pi_{13} - C_9 - C_{10} - C_{13} - C_{14}) = -E_{10} - E_{14} \\
\sigma_{13}^3 &= \frac{1}{2}(\pi_{13} - C_{11} - C_{12} - C_{15} - C_{16}) = -e^2 - e^3 + e_2 - e_3 + E_{11} + E_{15} \\
\sigma_{13}^4 &= \frac{1}{2}(\pi_{13} - C_3 - C_4 - C_7 - C_8) = -e^2 - e^3 + E_3 + E_7 \quad (60)
\end{aligned}$$

$$\begin{aligned}
\sigma_{42}^1 &= \frac{1}{2}(\pi_{42} - C_6 - C_8 - C_{13} - C_{15}) = e_2 - e_3 - e^3 - E_5 - E_6 + E_{13} + E_{15} \\
\sigma_{42}^2 &= \frac{1}{2}(\pi_{42} - C_5 - C_7 - C_{14} - C_{16}) = -e^3 + e_2 - e_3 - E_6 - E_8 + E_{15} + E_{16} \\
\sigma_{42}^3 &= \frac{1}{2}(\pi_{42} - C_2 - C_4 - C_9 - C_{11}) = e_1 + e_2 - e_3 - e^3 \\
&\quad + \frac{1}{2}(E_1 - E_2 + E_3 - E_4 - E_5 - E_6 - E_7 - E_8) \\
&\quad + \frac{1}{2}(-E_9 - E_{10} + E_{11} + E_{12} + E_{13} + E_{14} + E_{15} + E_{16}) \\
\sigma_{42}^4 &= \frac{1}{2}(\pi_{42} - C_1 - C_3 - C_{10} - C_{12}) = -e_1 + e_2 - e_3 - e^3 \\
&\quad + \frac{1}{2}(-E_1 - E_2 + E_3 + E_4 - E_5 - E_6 - E_7 - E_8) \\
&\quad + \frac{1}{2}(E_9 - E_{10} + E_{11} - E_{12} + E_{13} + E_{14} + E_{15} + E_{16}). \quad (61)
\end{aligned}$$

## References

- [1] F. Denef, “Les Houches Lectures on Constructing String Vacua,” arXiv:0803.1194 [hep-th].
- [2] R. Donagi and M. Wijnholt, “Model Building with F-Theory,” [arXiv:0802.2969 [hep-th]]; “Higgs Bundles and UV Completion in F-Theory,” arXiv:0904.1218 [hep-th].
- [3] C. Beasley, J. J. Heckman and C. Vafa, “GUTs and Exceptional Branes in F-theory - I,” [arXiv:0802.3391 [hep-th]]; “GUTs and Exceptional Branes in F-theory - II: Experimental Predictions,” [arXiv:0806.0102 [hep-th]]
- [4] A. Collinucci, F. Denef and M. Esole, “D-brane Deconstructions in IIB Orientifolds,” JHEP **0902** (2009) 005 [arXiv:0805.1573 [hep-th]].
- [5] R. Blumenhagen, V. Braun, T. W. Grimm and T. Weigand, “GUTs in Type IIB Orientifold Compactifications,” Nucl. Phys. B **815** (2009) 1 [arXiv:0811.2936 [hep-th]].
- [6] B. Andreas and G. Curio, “From Local to Global in F-Theory Model Building,” arXiv:0902.4143 [hep-th].
- [7] J. Marsano, N. Saulina and S. Schafer-Nameki, “F-theory Compactifications for Supersymmetric GUTs,” arXiv:0904.3932 [hep-th]; “Monodromies, Fluxes, and Compact Three-Generation F-theory GUTs,” arXiv:0906.4672 [hep-th].
- [8] R. Blumenhagen, J. P. Conlon, S. Krippendorf, S. Moster and F. Quevedo, “SUSY Breaking in Local String/F-Theory Models,” arXiv:0906.3297 [hep-th].
- [9] A. Collinucci, “New F-theory lifts,” arXiv:0812.0175 [hep-th]; “New F-theory lifts II: Permutation orientifolds and enhanced singularities,” arXiv:0906.0003 [hep-th].
- [10] R. Blumenhagen, T. W. Grimm, B. Jurke and T. Weigand, “F-theory uplifts and GUTs,” arXiv:0906.0013 [hep-th].
- [11] S. G. Nibbelink, D. Klevers, F. Ploger, M. Trapletti and P. K. S. Vaudrevange, “Compact heterotic orbifolds in blow-up,” JHEP **0804** (2008) 060 [arXiv:0802.2809 [hep-th]].



- [12] G. Honecker and M. Trapletti, “Merging heterotic orbifolds and K3 compactifications with line bundles,” JHEP **0701** (2007) 051 [arXiv:hep-th/0612030];
- [13] S. G. Nibbelink, M. Trapletti and M. Walter, “Resolutions of  $C^n/Z_n$  Orbifolds, their U(1) Bundles, and Applications to String Model Building,” JHEP **0703** (2007) 035 [arXiv:hep-th/0701227];
- [14] S. Groot Nibbelink, H. P. Nilles and M. Trapletti, “Multiple anomalous U(1)s in heterotic blow-ups,” Phys. Lett. B **652** (2007) 124 [arXiv:hep-th/0703211];
- [15] S. G. Nibbelink, T. W. Ha and M. Trapletti, “Toric Resolutions of Heterotic Orbifolds,” Phys. Rev. D **77** (2008) 026002 [arXiv:0707.1597 [hep-th]].
- [16] P. S. Aspinwall, “K3 surfaces and string duality,” arXiv:hep-th/9611137.
- [17] P. S. Aspinwall and J. Louis, Phys. Lett. B **369** (1996) 233 [arXiv:hep-th/9510234].
- [18] P. S. Aspinwall, “M-theory versus F-theory pictures of the heterotic string,” Adv. Theor. Math. Phys. **1** (1998) 127 [arXiv:hep-th/9707014].
- [19] W. Barth, C. Peters and A. Van de Ven, Compact complex surfaces, Ergeb. Math. Grenzgeb. (3) 4, Springer-Verlag, Berlin, 1984.
- [20] V. Alexeev and V. V. Nikulin, “Classification of log del Pezzo surfaces of index  $\leq 2$ ” [arXiv:math/0406536v6].
- [21] C. Vafa, “Evidence for F-Theory,” Nucl. Phys. B **469** (1996) 403 [arXiv:hep-th/9602022].
- [22] A. Sen, “Orientifold limit of F-theory vacua,” Nucl. Phys. Proc. Suppl. **68** (1998) 92 [Nucl. Phys. Proc. Suppl. **67** (1998) 81] [arXiv:hep-th/9709159].
- [23] R. Gopakumar and S. Mukhi, “Orbifold and orientifold compactifications of F-theory and M-theory to six and four dimensions,” Nucl. Phys. B **479**, 260 (1996) [arXiv:hep-th/9607057].
- [24] A. Klemm, B. Lian, S. S. Roan and S. T. Yau, “Calabi-Yau fourfolds for M- and F-theory compactifications,” Nucl. Phys. B **518** (1998) 515 [arXiv:hep-th/9701023].
- [25] P. Berglund, A. Klemm, P. Mayr and S. Theisen, “On type IIB vacua with varying coupling constant,” Nucl. Phys. B **558** (1999) 178 [arXiv:hep-th/9805189].

- [26] J. de Boer, R. Dijkgraaf, K. Hori, A. Keurentjes, J. Morgan, D. R. Morrison and S. Sethi, “Triples, fluxes, and strings,” *Adv. Theor. Math. Phys.* **4** (2002) 995 [arXiv:hep-th/0103170].
- [27] J. H. Conway and N. J. A. Sloane, *Sphere Packings, Lattices and Groups*, Berlin, Heidelberg and New York, 1988.
- [28] S. Helgason, *Differential Geometry and Symmetric Spaces*, Oxford University Press; (2001) .
- [29] K. S. Choi, K. Hwang and J. E. Kim, “Dynkin diagram strategy for orbifolding with Wilson lines,” *Nucl. Phys. B* **662**, 476 (2003) [arXiv:hep-th/0304243];
- [30] A. Hebecker and M. Ratz, “Group-theoretical aspects of orbifold and conifold GUTs,” *Nucl. Phys. B* **670**, 3 (2003) [arXiv:hep-ph/0306049].
- [31] E. B. Dynkin, “Semisimple subalgebras of semisimple Lie algebras,” *Trans. Am. Math. Soc.* **6**, 111 (1957).
- [32] R. Slansky, “Group Theory For Unified Model Building,” *Phys. Rept.* **79**, 1 (1981).
- [33] E. Witten, “String theory dynamics in various dimensions,” *Nucl. Phys. B* **443**, 85 (1995) [arXiv:hep-th/9503124].
- [34] V. V. Nikulin, “Discrete Reflection Groups in Lobachevsky Spaces and Algebraic Surfaces,” *Proceedings of the International Congress of Mathematicians*, edited by G. M. Gleason, Berkeley, 654 (1986).
- [35] D. Lust, S. Reffert, E. Scheidegger and S. Stieberger, “Resolved toroidal orbifolds and their orientifolds,” *Adv. Theor. Math. Phys.* **12** (2008) 67 [arXiv:hep-th/0609014].
- [36] P. Griffiths, J. Harris, “Principles of Algebraic Geometry”, Wiley-Interscience; (1994)
- [37] V. Kumar and W. Taylor, “Freedom and Constraints in the K3 Landscape,” arXiv:0903.0386 [hep-th].
- [38] A. Sen, “F-theory and Orientifolds,” *Nucl. Phys. B* **475** (1996) 562 [arXiv:hep-th/9605150].

- [39] A. P. Braun, A. Hebecker and H. Triendl, “D7-Brane Motion from M-Theory Cycles and Obstructions in the Weak Coupling Limit,” Nucl. Phys. B **800**, 298 (2008) [arXiv:0801.2163 [hep-th]].
- [40] A. Sen, “Orientifold limit of F-theory vacua,” Phys. Rev. D **55** (1997) 7345 [arXiv:hep-th/9702165].
- [41] A. Sen, “F-theory and the Gimon-Polchinski orientifold,” Nucl. Phys. B **498** (1997) 135 [arXiv:hep-th/9702061].
- [42] C. Borcea, “K3 Surfaces with Involution and Mirror Pairs of Calabi-Yau Manifolds,” *American Mathematical Society/International Press Studies in Advanced Mathematics, Mirror Symmetry II*, edited by B. Greene and S.-T. Yau, Cambridge (MA), 717 (1996).
- [43] A. P. Braun, A. Hebecker, C. Ludeling and R. Valandro, “Fixing D7 Brane Positions by F-Theory Fluxes,” Nucl. Phys. B **815** (2009) 256 [arXiv:0811.2416 [hep-th]].
- [44] R. Valandro, “Type IIB Flux Vacua from M-theory via F-theory,” JHEP **0903** (2009) 122 [arXiv:0811.2873 [hep-th]].
- [45] L. Gorlich, S. Kachru, P. K. Tripathy and S. P. Trivedi, “Gaugino condensation and nonperturbative superpotentials in flux compactifications,” JHEP **0412** (2004) 074 [arXiv:hep-th/0407130]
- [46] D. Lust, P. Mayr, S. Reffert and S. Stieberger, “F-theory flux, destabilization of orientifolds and soft terms on D7-branes,” Nucl. Phys. B **732**, 243 (2006) [arXiv:hep-th/0501139]
- [47] K. Dasgupta, G. Rajesh and S. Sethi, “M theory, orientifolds and G-flux,” JHEP **9908** (1999) 023 [arXiv:hep-th/9908088]
- [48] P. S. Aspinwall and R. Kallosh, “Fixing all moduli for M-theory on K3 x K3,” JHEP **0510**, 001 (2005) [arXiv:hep-th/0506014]